Ephemeris refinement of 21 Hot Jupiter exoplanets with high timing uncertainties

Journal Item

A&A 622, A81 (2019)
https://doi.org/10.1051/0004-6361/201834194

Astronomy & Astrophysics

Ephemeris refinement of 21 hot Jupiter exoplanets with high timing uncertainties*

M. Mallonn[1], C. von Essen[2], E. Herrero[3,4], X. Alexoudi[1], T. Granzer[1], M. Sosa[5,6], K. G. Strassmeier[1], G. Bakos[7,**], D. Bayliss[8], R. Brahm[9,10,11], M. Bretton[12], F. Campos[13], L. Carone[14], K. D. Colón[15], H. A. Dale[16], D. Dragomir[17,***], N. Espinoza[14,****,†], P. Evans[18], F. Garcia[19], S.-H. Gu[20,21,22], P. Guerra[23], Y. Jongen[24], A. Jordán[9,11,14], W. Kang[25], E. Keles[1], T. Kim[25], M. Lendl[26,14], D. Molina[27], M. Salisbury[28], F. Scaggiante[29], A. Shporer[17], R. Siverd[30], E. Sokov[31,32], I. Sokova[32], and A. Wünsche[12]

(Affiliations can be found after the references)

Received 8 November 2018 / Accepted 14 December 2018

ABSTRACT

Transit events of extrasolar planets offer a wealth of information for planetary characterization. However, for many known targets, the uncertainty of their predicted transit windows prohibits an accurate scheduling of follow-up observations. In this work, we refine the ephemerides of 21 hot Jupiter exoplanets with the largest timing uncertainties. We collected 120 professional and amateur transit light curves of the targets of interest, observed with a range of telescopes of 0.3 m–2.2 m, and analyzed them along with the timing information of the planets discovery papers. In the case of WASP-117b, we measured a timing deviation compared to the known ephemeris of about 3.5 h, and for HAT-P-29b and HAT-P-31b the deviation amounted to about 2 h and more. For all targets, the new ephemeris predicts transit timings with uncertainties of less than 6 min in the year 2018 and less than 13 min until 2025. Thus, our results allow for an accurate scheduling of follow-up observations in the next decade.

Key words. methods: observational – techniques: photometric – planets and satellites: fundamental parameters

1. Introduction

The transit of an extrasolar planet delivers a wealth of information. Time-series photometry of the event allows for the derivation of the orbital period, the orbital inclination, and the planet-star radius ratio (Charbonneau et al. 2000; Seager & Mallén-Ornelas 2003). If the host star is well characterized by high-resolution spectroscopy, a radial velocity curve by a spectroscopic time-series offers the mass of the transiting system (e.g., Bouchy et al. 2005). This mass in combination with the transit information yields the mean density of the planet. Transiting systems also provide information on their atmospheric composition through transmission spectroscopy, information on the thermal energy budget through emission spectroscopy, and allow for conclusions on their migration history through the measurement of the misalignment of stellar spin and planetary orbit in accordance with the Rossiter-McLaughlin effect (e.g., Wakeford et al. 2017; Arcangeli et al. 2018; Albrecht et al. 2012).

However, any follow-up observation of the transit events, either with photometry, low or high-resolution spectroscopy, or even with polarimetry, relies on reasonably accurate knowledge of the timing of the transit. This knowledge degrades over time because the timing uncertainty increases linearly with the number of transit epochs that have passed since the last observation. The large number of exoplanets discovered per year nowadays makes it more and more difficult to ensure parameter refinement studies for all targets. Therefore, there is a non-negligible number of systems for which the timing uncertainty has reached values of 30 min or more. This uncertainty is too high for follow-up observations with space-based or large ground-based telescopes, where observing time is very expensive and good coverage of out-of-transit observations cannot be guaranteed within a limited observing interval. The timing uncertainty can grow so much that the knowledge of when the transit happens is practically lost. Current examples are CoRoT-24b and c (Alonso et al. 2014).

The goal of this work is to refine the ephemeris information of hot Jupiter systems that exhibit large timing uncertainties to ensure the possibility of future follow-up observations. In Sect. 2, we describe our target selection, in Sect. 3 we provide details about the observations for this work, and in Sect. 4 we explain the data analysis. Section 5 provides the results, Sect. 6 gives a discussion, and in Sect. 7 we finish the paper by outlining our conclusions.

2. Target selection

We compiled a target list with the ephemeris information of hot Jupiter exoplanets from the NASA Exoplanet Archive (Akeson et al. 2013) and calculated the transit time uncertainty by mid 2018. We constrained our target selection to the planets discovered by ground-based surveys and include all planets named with the prefix WASP, HAT-P, HATS, XO, TrES, KELT, Qatar, and MASCARA. We noticed that several planets discovered by the space mission CoRoT, next to the aforementioned CoRoT-24 b and c, have a timing uncertainty above 30 min; examples are CoRoT-16b and 17b with three- and six-hour transit timing uncertainty. However, due to their relative faintness

* Observational lightcurves are only available at the CDS via anonymous ftp to cdsarc.u-strasbg.fr (130.79.128.5) or via http://cdsarc.u-strasbg.fr/viz-bin/qcat?J/A+A/622/A81

** MTA Distinguished Guest Fellow, Konkoly Observatory.

*** NASA Hubble Fellow.

**** Bernoulli Fellow.

† Gruber Fellow.

of about fifteenth magnitude in Johnson V, these targets are of limited value for detailed characterization and generally of less interest for follow-up observations. Hence, they are not included here. From the general formula of a planet ephemeris,

$$T_c = T_0 + n \cdot P, \quad (1)$$

with T_0 as the timing zero point, P as the orbital period, and n as the number of epochs passed since T_0, we calculate the uncertainty of the calculated timing T_c according to the general rules of uncertainty propagation:

$$\Delta T = \sqrt{\Delta T_0^2 + (n \cdot \Delta P)^2}. \quad (2)$$

This equation does not take into account a potential covariance of T_0 and P, however, for those of our targets with the largest timing uncertainties, ΔT is strongly dominated by the term $n \cdot \Delta P$ and a potential covariance is of minor importance.

For the 267 targets in our list, the timing uncertainty by August 2018 ranges from 0.3 min to 172 min with a median of 4 min. For the 50 objects with the largest timing uncertainties, we verified that the used ephemeris values were still up to date by checking for each individual target the publications listed in *The Extrasolar Planets Encyclopaedia* (Schneider et al. 2011) under "Related Publications" and by checking all publications that cited the discovery paper of the target of interest.

At the time of target selection and data acquisition of this project, HAT-P-25b and HAT-P-38b were ranked position 11 and 8 in Table 1 with timing uncertainties of 23.7 and 24.6 min according to their discovery papers Quinn et al. (2012) and Sato et al. (2012). In the course of this work, the ephemerides of these planets were improved by Wang et al. (2018b) and Bruno et al. (2018). Both targets are still included here as a consistency check with the new values. For the three hot Jupiters Qatar-3b, -4b, and -5b, the orbital period uncertainty was not provided in their discovery paper Alsubai et al. (2017). These planets are included here for a new analysis because new results published at the *Exoplanet Transit Database* (ETD, Poddaný et al. 2010) indicate deviations from the currently known ephemerides for two of the three targets. We finish the ranking in Table 1 at an uncertainty of 11 min. This value is rather arbitrary, but we consider uncertainties smaller than this value to cause only minor problems in the scheduling of transit follow-up observations.

The targets of our sample are very diverse in their planetary and stellar parameters, therefore they are of interest for a broad bandwidth of investigations: from investigations on radius inflation mechanisms of hot Jupiters (Qatar-4b and Kelt-8b have radii larger than 1.5 Jupiter radii) and tidal star-planet interactions (HAT-P-34b, Qatar-3b, Qatar-4b, and Qatar-5b have masses above 3 Jupiter masses), through studies on the formation history of the rare hot Jupiters with planetary companions (HAT-P-44b, HAT-P-45b, HAT-P-46b), to a search for mechanisms that excite the eccentricity of close-in gas giants (HAT-P-31b, HAT-P-34b, WASP-117b). Four host stars among the sample are peculiarly bright with $V < 10.5$ mag, simplifying any effort for follow-up. WASP-117b is one of the longest-period hot Jupiters and the orbit has been almost unchanged by tidal interaction during its lifetime (Lendl et al. 2014). Because of the large timing uncertainties of our targets, any effort for follow-up observations will greatly benefit from a prior ephemeris refinement.

Table 1. Ranking of hot Jupiter exoplanets according to their timing uncertainties as of August 2018.

Seq	Planet	ΔT_c (min)	Reference
1	**WASP-73b**	171.7	Delrez et al. (2014)
2	**WASP-117b**	143.1	Lendl et al. (2014)
3	**HAT-P-31b**	106.1	Kipping et al. (2011)
4	**KELT-8b**	103.8	Fulton et al. (2015)
5	**HAT-P-46b**	40.9	Hartman et al. (2014)
6	**HAT-P-29b**	38.8	Buchhave et al. (2011)
7	**HAT-P-45b**	25.2	Hartman et al. (2014)
8	KELT-10b	24.3	Kuhn et al. (2016)
9	**HAT-P-42b**	23.7	Boisse et al. (2013)
10	**HAT-P-35b**	22.9	Bakos et al. (2012)
11	WASP-99b	21.3	Hellier et al. (2014)
12	**HAT-P-44b**	16.8	Hartman et al. (2014)
13	**HAT-P-43b**	15.2	Boisse et al. (2013)
14	KELT-15b	14.1	Rodriguez et al. (2016)
15	**WASP-37b**	13.3	Simpson et al. (2011)
16	HAT-P-15b	13.2	Kovács et al. (2010)
17	**HAT-P-34b**	12.3	Bakos et al. (2012)
18	**HAT-P-52b**	12.2	Hartman et al. (2015)
19	**KELT-3b**	12.1	Pepper et al. (2013)
20	WASP-86/KELT-12b	11.6	Faedi et al. (2016)
21	**WASP-58b**	11.1	Hébrard et al. (2013)
121	**HAT-P-38b**	4.3	Bruno et al. (2018)
251	**HAT-P-25b**	0.9	Wang et al. (2018b)
	Qatar-3b		Alsubai et al. (2017)
	Qatar-4b		Alsubai et al. (2017)
	Qatar-5b		Alsubai et al. (2017)

Notes. The targets written in bold face are analyzed in this work.

3. Observations and data acquisition

Transit time-series photometry in the course of this work has been obtained with the 1.2-m STELLA telescope, the 0.8-m Joan Oró telescope (TJO) of the Montsec Astronomical Observatory, the 2.2-m telescope of the Calar Alto Observatory, the 2.15-m Jorge Sahade telescope (JST) of the Observatory Complejo Astronómico El Leoncito (CASLEO), the National Youth Space Center (NYSC) 1m telescope, the Chilean-Hungarian Automated Telescope (CHAT), a 1.0-m telescope of the Las Cumbres Observatory (LCO), and Yunnan.

STELLA and its wide-field imager WiFSIP (Strassmeier et al. 2004, 2010) observed 19 transits in total in the Sloan r' filter. The original field of view of WiFSIP of $22' \times 22'$ was reduced in all observations to $15' \times 15'$ to shorten the read-out time. A mild defocus was always applied to spread the PSF to an artificial FWHM of about $3''$.

Five transit light curves in Johnson V filter were obtained with the TJO and its main imager MEIA2. The instrument has a field of view of 12.3×12.3 arcmin and a resolution of 0.36 arcsec pixel^{-1}. All TJO observations employed the Johnson V filter.

One transit light curve was observed with the Calar Alto 2.2 m telescope and its instrument CAFOS in imaging mode. The SITe CCD chip was binned by 2×2 pixels. Additionally, we applied a read-out window to reduce the read-out time. A mild defocus was applied.

We observed one primary transits of WASP-73b with the JST. The observations were carried out using an R filter and binning 1×1. To increase the size of the field of view to an unvignetted 9 arcmin radius, we employed a focal reducer.

Five transits were obtained with the NYSC 1 m telescope at Deukheung Optical Astronomy Observatory (DOAO) in South Korea with either a FLI PL-16803 CCD camera or a Princeton Instruments SOPHIA-2048B CCD. The telescope was slightly defocused during the observations, and we employed a Cousins R filter.

Two transit light curves were observed with the CHAT, which is a newly commissioned 0.7 telescope at Las Campanas Observatory, Chile, built by members of the HATSouth (Bakos et al. 2013) team, and dedicated to the follow-up of transiting exoplanets. A more detailed account of the CHAT facility will be published at a future date (Jordán et al., in prep.[1]). Data were obtained with a Finger Lakes Microline CCD camera equipped with a back-illuminated CCD and a Sloan i′ filter. The camera, which has a field of view of $\approx 21' \times 21'$, was slightly defocused during the observations.

A light curve of WASP-117b transit was obtained in July 2017 at the LCO, which is a fully robotic network of telescopes (Brown et al. 2013), deployed around the globe in both hemispheres[2]. We used a 1.0-m telescope of the network at the South African Astrophysical Observatory (SAAO) and the Sinistro camera. The telescope was defocused by 3.0 mm.

One transit light curve was obtained with 1-m telescope of Yunnan Observatories, China, and its $2K \times 2K$ CCD camera using the Cousins R filter. The instrument offers a field of view of $7.2' \times 7.2'$ and a resolution of 0.2 arcsec pixel^{-1}.

We complemented our data sample with a large number of amateur light curves, which we obtained from the ETD[3] (Poddaný et al. 2010). We selected 85 light curves from this database by visual inspection. While the ETD offers an online fitting routine and provides the derived transit parameter, we downloaded the reduced light curves and re-analyzed them for their timing information homogeneously to the newly obtained light curves with professional telescopes (see Sect. 4). A summary of all 120 light curves and their properties is given in Table B.1.

Since the data of this paper were obtained by more than 30 different observatories, we did not attempt a homogeneous data reduction. The ETD observers uploaded reduced light curves to the online database and provided some details of the data reduction. The data reduction and light curve extraction of the professional observatories is briefly described in Appendix A.

All 120 light curves together with their transit fit (Sect. 4) are shown in Fig. B.1.

4. Light-curve analysis

In this work, we analyzed the photometric transit light curves with the publicly available software tool JKTEBOP (Southworth et al. 2004; Southworth 2008). Fit parameters were the orbital semi-major axis scaled by the stellar radius $a/R_\star$, the orbital inclination i, the planet-star radius ratio k, the midpoint of the transit T, the orbital period P, the eccentricity of the orbit e, the argument of periastron ω, and coefficients of the detrending function $c_{0,1,2}$.

Many studies suggest that trends in small-telescope transit photometry of 1–2 mmag photometric precision is fit by simple detrending functions with very few coefficients (e.g., Juvan et al. 2018; Southworth et al. 2016; Mancini et al. 2016; Maciejewski et al. 2016). For STELLA/WiFSIP photometry, several studies used the Bayesian Information Criterion to show that first or second order polynomials over time form the best representation of trends or systematics in the light curves (e.g., Mallonn et al. 2015, 2016; Mackebrandt et al. 2017). Therefore, and for the reason that the ETD light curves are lacking the information of external parameters for a more complex detrending, we detrended all light curves of this work consistently by a simple second-order polynomial over time. For the vast majority of targets we present a multiplicity of light curves which warrants a consistency check.

Crucial for the final derivation of robust uncertainties on the transit timing measurement is a reliable estimation of the photometric uncertainties. We started with the values delivered by the different aperture photometry software tools, which generally include the photon noise of the target, ensemble of comparison stars and background. We ran an initial transit model fit, subtracted the best fit model from the data, and performed a 4-σ clipping on the residuals to remove outliers. As a second step, we ran another transit fit and multiplied the photometric uncertainties by a common factor that results in a reduced χ^2 of unity for the fit. Additionally, we calculated the so-called β factor, a concept introduced by Gillon et al. (2006) and Winn et al. (2008) to include the contribution of correlated noise in the light curve analysis. It describes the evolution of the standard deviation σ of the light-curve residuals when they become binned in comparison to Poisson noise. In the presence of correlated noise, σ of the binned residuals is larger by the factor β than the binned uncorrelated (white) noise that decreases by the square root of the number of points per bin width. The value of β depends on the bin width, we use here the average of ten binning steps from half to twice the duration of ingress. We enlarged the photometric uncertainty finally by this factor β.

The dates of all light curves were converted to BJD_{TDB} (Eastman et al. 2010). All individual transit light curves were now fit with i, $a/R_\star$, k, P, e, and ω fixed to literature values. In the case of HAT-P-29b, we used the updated parameter values of Wang et al. (2018a). The limb darkening coefficients of the quadratic law were fixed to theoretical values from Claret et al. (2012, 2013) according to their stellar parameters obtained from the planet discovery papers. ETD light curves taken with a Clear filter were fit with limb darkening coefficients according to Cousins R. The free-to-fit parameters for each individual light curve were T and $c_{0,1,2}$. All individual transit mid-times are summarized in Table B.2.

The estimation of the transit parameter uncertainties was done in JKTEBOP with a Monte Carlo simulation (Southworth et al. 2005), and with a residual-permutation algorithm that takes correlated noise into account (Southworth 2008). The Monte Carlo simulation was run with 5000 steps. As final parameter uncertainties we adopted the larger value of both methods. The uncertainties of the fixed transit parameters were included in the final timing uncertainty by letting them vary during the error estimation within the 1-σ ranges of the literature values.

In the final step, we performed a joint fit of all light curves per target and included T_0 with its uncertainty of the previous ephemeris of the discovery paper. Free-to-fit values were P and T_0 of a new ephemeris and the detrending coefficients $c_{0,1,2}$ per light curve. The epoch of T_0 was chosen to minimize the covariance between T_0 and P. In the cases of HAT-P-25b and HAT-P-38b, for which refined ephemerides were published in the course of our analysis, we included also the individual transit times that became available (see Table B.2). The new ephemerides of the 21 exoplanets of this work are summarized in Table 2. In Figs. B.2–B.4, we show the individual observed-minus-calculated timing deviations. For HAT-P-29b,

[1] https://www.exoplanetscience2.org/sites/default/files/submission-attachments/poster_aj.pdf
[2] For updated information about the network, see: https://lco.global
[3] http://var2.astro.cz/ETD; http://var2.astro.cz/tresca

Table 2. Refined ephemerides resulting from this work.

Planet	T_0 [BJD_TDB]	P (days)	Reference
HAT-P-25b	2455176.85173 ± 0.00047	3.652836 ± 0.000019	Quinn et al. (2012)
	2456418.80996 ± 0.00025	3.65281572 ± 0.00000095	Wang et al. (2018b)
	2457006.91299 ± 0.00021	3.65281591 ± 0.00000067	This work
HAT-P-29b	2455197.57617 ± 0.00181	5.723186 ± 0.000049	Buchhave et al. (2011)
	2456170.5494 ± 0.0015	5.723390 ± 0.000013	Wang et al. (2018a)
	2457092.00345 ± 0.00128	5.7233773 ± 0.0000072	This work
HAT-P-31b	2454320.8866 ± 0.0051	5.005425 ± 0.000091	Kipping et al. (2011)
	2458169.9410 ± 0.0017	5.0052724 ± 0.0000063	This work
HAT-P-34b	2455431.59706 ± 0.00055	5.452654 ± 0.000016	Bakos et al. (2012)
	2456462.14718 ± 0.00053	5.4526470 ± 0.0000031	This work
HAT-P-35b	2455578.66158 ± 0.00050	3.646706 ± 0.000021	Bakos et al. (2012)
	2456836.75811 ± 0.00041	3.6466566 ± 0.0000012	This work
HAT-P-38b	2455863.12034 ± 0.00035	4.640382 ± 0.000032	Sato et al. (2012)
		4.6403294 ± 0.0000055	Bruno et al. (2018)
	2457491.87585 ± 0.00009	4.6403293 ± 0.0000017	This work
HAT-P-42b	2455952.52683 ± 0.00077	4.641876 ± 0.000032	Boisse et al. (2013)
	2456036.07987 ± 0.00077	4.6418381 ± 0.0000080	This work
HAT-P-43b	2455997.37182 ± 0.00032	3.332687 ± 0.000015	Boisse et al. (2013)
	2456147.34248 ± 0.00030	3.3326830 ± 0.0000019	This work
HAT-P-44b	2455696.93772 ± 0.00024	4.301219 ± 0.000019	Hartman et al. (2014)
	2456204.47794 ± 0.00019	4.3011886 ± 0.0000010	This work
HAT-P-45b	2455729.98689 ± 0.00041	3.128992 ± 0.000021	Hartman et al. (2014)
	2456502.84809 ± 0.00033	3.1289923 ± 0.0000014	This work
HAT-P-46b	2455701.33723 ± 0.00047	4.463129 ± 0.000048	Hartman et al. (2014)
	2455969.12547 ± 0.00044	4.4631365 ± 0.0000050	This work
HAT-P-52b	2455852.10403 ± 0.00041	2.7535953 ± 0.0000094	Hartman et al. (2015)
	2456645.13981 ± 0.00032	2.7535965 ± 0.0000011	This work
KELT-3b	2456034.29537 ± 0.00038	2.703390 ± 0.000010	Pepper et al. (2013)
	2456269.48987 ± 0.00029	2.7033850 ± 0.0000018	This work
KELT-8b	2456883.4803 ± 0.0007	3.24406 ± 0.00016	Fulton et al. (2015)
	2457396.04496 ± 0.00055	3.2440796 ± 0.0000048	This work
Qatar-3b	2457302.45300 ± 0.00010	2.5079204	Alsubai et al. (2017)
	2457312.48458 ± 0.00010	2.5078952 ± 0.0000032	This work
Qatar-4b	2457637.77361 ± 0.00046	1.8053564	Alsubai et al. (2017)
	2457872.47170 ± 0.00046	1.8053704 ± 0.0000042	This work
Qatar-5b	2457336.75824 ± 0.00010	2.8792319	Alsubai et al. (2017)
	2457362.67203 ± 0.00009	2.8793105 ± 0.0000025	This work
WASP-37b	2455338.6196 ± 0.0006	3.577469 ± 0.000011	Simpson et al. (2011)
	2456393.97698 ± 0.00052	3.5774807 ± 0.0000019	This work
WASP-58b	2455183.9342 ± 0.0010	5.017180 ± 0.000011	Hébrard et al. (2013)
	2457261.05970 ± 0.00062	5.0172131 ± 0.0000026	This work
WASP-73b	2456128.7063 ± 0.0011	4.08722 ± 0.00022	Delrez et al. (2014)
	2456365.7688 ± 0.0011	4.0872856 ± 0.0000087	This work
WASP-117b	2456533.82404 ± 0.00095	10.02165 ± 0.00055	Lendl et al. (2014)
	2457355.51373 ± 0.00055	10.020607 ± 0.000011	This work

Wang et al. (2018a) found the T_0 provided in the discovery paper (Buchhave et al. 2011) to be affected by an overly small value of the transit duration. Therefore, we used the corrected timings from Wang et al. (2018a) in the joint fit. As a consequence, there is an offset between the displayed previous ephemeris and the corresponding corrected timing values (Fig. B.2, upper right panel) of the discovery paper.

We do not attempt a refinement of transit parameters in addition to the ephemerides because a significant fraction of the light curves used here either miss parts of the transit event or do not reach millimag-precision. However, the light curves are available at the Strasbourg astronomical Data Center (CDS) for further use.

5. Results

5.1. Ephemeris refinement of 21 exoplanets

We use the recently published, refined ephemeris values for HAT-P-25b and HAT-P-38b as a cross-check for the values derived in this work. For both planets, the periods deviate only by fractions of the 1-σ uncertainties compared to the refined values of Wang et al. (2018b) and Bruno et al. (2018). We were able to increase the precision of the orbital period estimation because we extended the covered time span by one more season. At a late stage in the preparation of this publication, a follow-up study for HAT-P-29b became available (Wang et al. 2018a). We also reached an agreement for the ephemeris within 1-σ for this latter work.

For all individual timings of this study over all targets, we calculate the reduced χ^2 value to be about 1.1. This indicates a reasonable good match between the average deviation from the corresponding linear ephemeris and the measurement uncertainty. A $\chi^2_{\rm red}$ slightly larger than unity can be caused by starspots in the host-star photosphere that deform the shape of photometric transit curve (Oshagh et al. 2013; Holczer et al. 2015).

For the majority of the targets investigated in this work, the photometric quality of the light curves only allowed for a slight improvement on the precision of T_0 compared to the discovery papers. However, including the timing measurement of these publications, our data expand the time interval of observed transit events for all targets significantly. Therefore, the uncertainty of the estimated orbital period P could be lowered by an order of magnitude for all targets. Objects worth emphasizing are WASP-117b, HAT-P-31b, and HAT-P-29b, for which we measured the predicted transit times to be off by more than 2 h. For WASP-117b, the actual deviation amounted to about 3.5 h. In the case of HAT-P-35b and WASP-73b, the difference between prediction and measurement was on the order of 1 hour. For HAT-P-29b, the measured timings deviated by 3.7σ from the ephemeris given in the discovery paper.

5.2. Comparison to the ETD online fit results

The Exoplanet Transit Database performs a transit fit to the uploaded light curves (Poddaný et al. 2010). The achieved best fit parameters are listed on the webpage and are regularly used in scientific publications (e.g., Southworth et al. 2016; Angerhausen et al. 2017; Lillo-Box et al. 2018). Our reanalyzed timing values of 85 ETD light curves allow for a cross check with these ETD results. We find that on average the absolute timing shows a deviation of only 20% of our 1-σ error bars; that is, there is no systematic offset. However, there is a significant scatter of the individual timing differences with a standard deviation of one when expressed in terms of our derived 1-σ uncertainties. In extreme cases, the deviations between our best-fit values and ETD derived parameters reached 4σ. We find that the ETD error bars are on average smaller by a factor of 1.7 than the corresponding values derived by the standard procedures used in this work. The ETD adopts the parameter uncertainties from a Levenberg–Marquardt optimization algorithm (Poddaný et al. 2010), which is believed to be unreliable in the presence of parameter correlations (see Southworth 2008, and references therein). Therefore, we recommend the re-analysis of ETD light curves instead of the usage of the transit parameters obtained by the online fitting tool.

6. Discussion

We use our sample of 21 newly determined ephemerides to check statistically if the differences between old and new ephemerides are in general agreement to the previous ephemeris uncertainties. When we express the measured-to-predicted timing deviation of all our 21 targets in units of their previously known timing uncertainties, we find a standard deviation for all targets of about 1.4 one-sigma uncertainties; that is, larger than unity. This indicates a trend of slightly underestimated uncertainties of the ephemerides. There may be various reasons for this depending on individual targets; for example, underestimated systematics in the data, systematic effects on the host star, like stellar activity, or transit timing variations (TTV).

We consider it to be possible that significant timing deviations from the predicted values originate from TTVs. Such variation could be caused by gravitational interactions of the observed hot Jupiter with unknown planetary companions (von Essen et al. 2018, and references therein). Hot Jupiter planets are known to mostly orbit their host star alone (Steffen et al. 2012). However in recent years a few exceptions to this general rule have been found, such as the planetary system of WASP-47 with one hot Jupiter accompanied by an interior and an exterior sub-Neptune (Becker et al. 2015; Neveu-VanMalle et al. 2016). Using all 3.5 years of Kepler spacecraft data, Huang et al. (2016) showed that these exceptions are very rare. For two of these systems, HAT-P-13 and WASP-47, the literature provides constraints on the TTV amplitude caused by the companions. In the case of HAT-P-13b, Fulton et al. (2011) ruled out periodic TTV of an amplitude larger than 144 s, while for WASP-47b, Becker et al. (2015) measured a TTV amplitude of 38 s. The planetary systems of the hot Jupiters WASP-53b and WASP-81b are uncommon in that they also each harbor an eccentric brown dwarf within a few astronomical units of the host star. Predicted TTVs of these hot Jupiters are below 1 min (Triaud et al. 2017).

Among our target list, there are three systems with RV candidate signals of Jupiter-mass companions within 1 AU, HAT-P-44, HAT-P-45, and HAT-P-46 (Hartman et al. 2014). Our newly derived ephemerides of HAT-P-45b and HAT-P-46b are in very good agreement with the ones previously published by Hartman et al. (2014). The individual data points from different seasons show no significant deviation from the linear ephemerides, and therefore we find no indications for significant effects of TTVs. On the other hand, the eight individual measurements of HAT-P-44b show a rather large reduced χ^2 value of 2.3. Nevertheless, we find no TTV periodicity at the planet companion period of about 220 days. The newly derived value of the period deviates by about 25 min from the discovery paper. To compute an order of magnitude of the amplitude of TTVs of planet b caused by the outer perturber, we made use of *TTVFast* (Deck et al. 2014). Here we assumed coplanar orbits, a circular orbit for the perturber, and the masses and periods from Hartman et al. (2014). The derived TTV amplitude for planet HAT-P-44b is about 6 s, which is extremely challenging to measure for ground-based observatories. With increasing mutual inclination, the mass of the outer perturber would also increase due to the degeneracy of M with $\sin i$, and so would the TTV amplitude (Payne & Ford 2011). However, we consider it to be likely that TTVs only have a marginal effect on the deviation of 25 min. It is more probable that this deviation is caused by the limited precision of the previous ephemeris, since it amounts to only 1.6σ, which we do not consider as significant.

An indicator for the potential existence of an outer perturber causing TTVs might also be a nonzero eccentricity of the hot Jupiter. Among our target list, there are four targets with an e significantly different from zero: WASP-117b, HAT-P-29b, HAT-P-31b, and HAT-P-34b. For all four targets, both the number of individual transit epochs and their individual precision is too low to allow for conclusions on TTVs with approximately one-minute amplitudes. We increase the precision of the period determination by an order of magnitude, and therefore our new ephemerides form the best available basis for future follow-up studies.

The target HAT-P-29b shows the most significant deviation of measured-to-predicted transit timings with a significance level of 3.7, a deviation very recently also described by Wang et al. (2018a). In this particular case, a likely explanation is the sensitivity of the used partial transit light curves to an overly small value of the transit duration derived in the discovery paper. For more details, we point the reader to the discussion supplied in Wang et al. (2018a).

7. Conclusion

We have refined the ephemerides of 21 exoplanets which previously had the largest timing uncertainties of ground-based detected hot Jupiters. We made use of a total of 120 transit light curves: 35 obtained from professional observatories and 85 from amateur observers. The bulk of our data might be considered as data of only moderate photometric quality, since more than half of our light curves have a point-to-point scatter larger than 3 mmag, or lack the ingress or egress part of the transit. However, the present work is a valuable example of where light curves of small-sized telescopes can still play a crucial role in modern science. All data were analyzed homogeneously, and resulted in an increased precision in the estimations of the orbital periods by one order of magnitude when combined with the transit-timing information of the discovery papers. Previous to our work, the timing uncertainty of the 21 analyzed objects ranged from 11 to 171 min. We were able to lower this to values ranging from 1 to 6 min, and thus to ensure a reasonable scheduling of follow-up studies at least until the year 2025, when the timing uncertainties will still be below 12 min for all our targets. Our new ephemerides might be affected to a certain extent by stellar activity and TTVs caused by unknown companions. The former constitutes a form of correlated noise in the data and is accounted for in the error estimation, while the latter is less likely because additional companions to hot Jupiters are extremely rare and cause TTV of low amplitude. In any case, we emphasize that even in the cases of ephemerides affected by astrophysical disturbances, our new ephemerides present the best available basis for future follow-up studies. Currently, the ground-based detected hot Jupiter with the largest timing uncertainty is KELT-10b with $\Delta T_c \approx 24$ min (by August 2018). We note that especially due to the enormous effort of the observers of the Exoplanet Transit Database, there is currently no hot Jupiter known in the northern hemisphere discovered by ground-based surveys with a timing uncertainty larger than 14 min.

Acknowledgements. E.H. acknowledges support by the Spanish Ministry of Economy and Competitiveness (MINECO) and the Fondo Europeo de Desarrollo Regional (FEDER) through grant ESP2016-80435-C2-1-R, as well as the support of the Generalitat de Catalunya/CERCA program. D. D. acknowledges support provided by NASA through Hubble Fellowship grant HST-HF2-51372.001-A awarded by the Space Telescope Science Institute, which is operated by the Association of Universities for Research in Astronomy, Inc., for NASA, under contract NAS5-26555. E.S. acknowledges support by the Russian Science Foundation grant No. 14-50-00043 for conducting international photometric observing campaign. I.S. acknowledges support by the Russian Foundation for Basic Research (project No. 17-02-00542). R.B. acknowledges support from FONDECYT Post-doctoral Fellowship Project No. 3180246. M.L. acknowledges support from the Austrian Research Promotion Agency (FFG) under project 859724 "GRAPPA". S.-H.G. acknowledges the financial support from the National Natural Science Foundation of China (No.U1531121). L.C. recognizes funding from DLR – 50OR1804. Funding for the Stellar Astrophysics Centre is provided by The Danish National Research Foundation (Grant agreement no.: DNRF106). We thank the staff at the various participating observatories STELLA, CASLEO, Calar Alto, TJO, and others for their support. Partly based on data obtained with the STELLA robotic telescopes in Tenerife, an AIP facility jointly operated by AIP and IAC, on data acquired at Complejo Astronómico El Leoncito, operated under agreement between the Consejo Nacional de Investigaciones Científicas y Técnicas de la República Argentina and the National Universities of La Plata, Córdoba and San Juan, on observations collected at the Centro Astronómico Hispano Alemán (CAHA) at Calar Alto, operated jointly by the Max-Planck Institut für Astronomie and the Instituto de Astrofísica de Andalucía (CSIC), and on data obtained with the Joan Oró Telescope (TJO) of the Montsec Astronomical Observatory (OAdM), owned by the Generalitat de Catalunya and operated by the Institute for Space Studies of Catalonia (IEEC). This research has made use of the SIMBAD data base and VizieR catalog access tool, operated at CDS, Strasbourg, France, and of the NASA Astrophysics Data System (ADS).

References

Akeson, R. L., Chen, X., Ciardi, D., et al. 2013, PASP, 125, 989
Albrecht, S., Winn, J. N., Johnson, J. A., et al. 2012, ApJ, 757, 18
Alonso, R., Moutou, C., Endl, M., et al. 2014, A&A, 567, A112
Alsubai, K., Mislis, D., Tsvetanov, Z. I., et al. 2017, AJ, 153, 200
Angerhausen, D., Dreyer, C., Placek, B., et al. 2017, A&A, 608, A120
Arcangeli, J., Désert, J.-M., Line, M. R., et al. 2018, ApJ, 855, L30
Bakos, G. Á., Hartman, J. D., Torres, G., et al. 2012, AJ, 144, 19
Bakos, G. Á., Csubry, Z., Penev, K., et al. 2013, PASP, 125, 154
Becker, J. C., Vanderburg, A., Adams, F. C., Rappaport, S. A., & Schwengeler, H. M. 2015, ApJ, 812, L18
Bertin, E., & Arnouts, S. 1996, A&AS, 117, 393
Boisse, I., Hartman, J. D., Bakos, G. Á., et al. 2013, A&A, 558, A86
Bouchy, F., Udry, S., Mayor, M., et al. 2005, A&A, 444, L15
Brown, T. M., Baliber, N., Bianco, F. B., et al. 2013, PASP, 125, 1031
Bruno, G., Lewis, N. K., Stevenson, K. B., et al. 2018, AJ, 155, 55
Buchhave, L. A., Bakos, G. Á., Hartman, J. D., et al. 2011, ApJ, 733, 116
Charbonneau, D., Brown, T. M., Latham, D. W., & Mayor, M. 2000, ApJ, 529, L45
Claret, A., Hauschildt, P. H., & Witte, S. 2012, A&A, 546, A14
Claret, A., Hauschildt, P. H., & Witte, S. 2013, A&A, 552, A16
Colome, J., & Ribas, I. 2006, IAU Special Session, 6, 11
Deck, K. M., Agol, E., Holman, M. J., & Nesvorný, D. 2014, ApJ, 787, 132
Delrez, L., Van Grootel, V., Anderson, D. R., et al. 2014, A&A, 563, A143
Eastman, J., Siverd, R., & Gaudi, B. S. 2010, PASP, 122, 935
Faedi, F., Gómez Maqueo Chew, Y., Pollacco, D., et al. 2016, ArXiv e-prints [arXiv:1608.04225]
Fulton, B. J., Shporer, A., Winn, J. N., et al. 2011, AJ, 142, 84
Fulton, B. J., Collins, K. A., Gaudi, B. S., et al. 2015, ApJ, 810, 30
Gillon, M., Pont, F., Moutou, C., et al. 2006, A&A, 459, 249
Hartman, J. D., Bakos, G. Á., Torres, G., et al. 2014, AJ, 147, 128
Hartman, J. D., Bhatti, W., Bakos, G. Á., et al. 2015, AJ, 150, 168
Hébrard, G., Collier Cameron, A., Brown, D. J. A., et al. 2013, A&A, 549, A134
Hellier, C., Anderson, D. R., Cameron, A. C., et al. 2014, MNRAS, 440, 1982
Holczer, T., Shporer, A., Mazeh, T., et al. 2015, ApJ, 807, 170
Huang, C., Wu, Y., & Triaud, A. H. M. J. 2016, ApJ, 825, 98
Juvan, I. G., Lendl, M., Cubillos, P. E., et al. 2018, A&A, 610, A15
Kipping, D. M., Hartman, J., Bakos, G. Á., et al. 2011, AJ, 142, 95
Kovács, G., Bakos, G. Á., Hartman, J. D., et al. 2010, ApJ, 724, 866
Kuhn, R. B., Rodriguez, J. E., Collins, K. A., et al. 2016, MNRAS, 459, 4281
Lendl, M., Triaud, A. H. M. J., Anderson, D. R., et al. 2014, A&A, 568, A81
Lillo-Box, J., Leleu, A., Parviainen, H., et al. 2018, A&A, 618, A42
Maciejewski, G., Dimitrov, D., Fernández, M., et al. 2016, A&A, 588, L6
Mackebrandt, F., Mallonn, M., Ohlert, J. M., et al. 2017, A&A, 608, A26
Mallonn, M., Nascimbeni, V., Weingrill, J., et al. 2015, A&A, 583, A138
Mallonn, M., Bernt, I., Herrero, E., et al. 2016, MNRAS, 463, 604
Mancini, L., Giordano, M., Mollière, P., et al. 2016, MNRAS, 461, 1053
Neveu-VanMalle, M., Queloz, D., Anderson, D. R., et al. 2016, A&A, 586, A93
Oshagh, M., Santos, N. C., Boisse, I., et al. 2013, A&A, 556, A19
Payne, M. J., & Ford, E. B. 2011, ApJ, 729, 98
Pepper, J., Siverd, R. J., Beatty, T. G., et al. 2013, ApJ, 773, 64
Poddaný, S., Brát, L., & Pejcha, O. 2010, New Astron., 15, 297
Quinn, S. N., Bakos, G. Á., Hartman, J., et al. 2012, ApJ, 745, 80
Rodriguez, J. E., Colón, K. D., Stassun, K. G., et al. 2016, AJ, 151, 138
Sato, B., Hartman, J. D., Bakos, G. Á., et al. 2012, PASJ, 64, 97
Schneider, J., Dedieu, C., Le Sidaner, P., Savalle, R., & Zolotukhin, I. 2011, A&A, 532, A79
Seager, S., & Mallén-Ornelas, G. 2003, ApJ, 585, 1038
Shporer, A., Zhou, G., Fulton, B. J., et al. 2017, AJ, 154, 188
Simpson, E. K., Faedi, F., Barros, S. C. C., et al. 2011, AJ, 141, 8
Southworth, J. 2008, MNRAS, 386, 1644

Southworth, J., Maxted, P. F. L., & Smalley, B. 2004, MNRAS, 351, 1277
Southworth, J., Smalley, B., Maxted, P. F. L., Claret, A., & Etzel, P. B. 2005, MNRAS, 363, 529
Southworth, J., Tregloan-Reed, J., Andersen, M. I., et al. 2016, MNRAS, 457, 4205
Steffen, J. H., Ragozzine, D., Fabrycky, D. C., et al. 2012, Proc. Natl. Acad. Sci., 109, 7982
Strassmeier, K. G., Granzer, T., Weber, M., et al. 2004, Astron. Nachr., 325, 527
Strassmeier, K. G., Granzer, T., Weber, M., et al. 2010, Adv. Astron., 2010, 970306
Triaud, A. H. M. J., Neveu-VanMalle, M., Lendl, M., et al. 2017, MNRAS, 467, 1714
von Essen, C., Ofir, A., Dreizler, S., et al. 2018, A&A, 615, A79
Wakeford, H. R., Sing, D. K., Kataria, T., et al. 2017, Science, 356, 628
Wang, X.-B., Gu, S.-H., Collier Cameron, A., et al. 2014, AJ, 147, 92
Wang, S., Wang, X.-Y., Wang, Y.-H., et al. 2018a, AJ, 156, 181
Wang, X.-Y., Wang, S., Hinse, T. C., et al. 2018b, PASP, 130, 064401
Winn, J. N., Holman, M. J., Torres, G., et al. 2008, ApJ, 683, 1076

---

[1] Leibniz-Institut für Astrophysik Potsdam, An der Sternwarte 16, 14482 Potsdam, Germany
e-mail: mmallonn@aip.de
[2] Stellar Astrophysics Centre, Department of Physics and Astronomy, Aarhus University, Ny Munkegade 120, 8000 Aarhus C, Denmark
[3] Institut de Ciéncies de l'Espai (ICE, CSIC), Campus UAB, Carrer de Can Magrans s/n, 08193 Cerdanyola del Vallès, Spain
[4] Institut d'Estudis Espacials de Catalunya (IEEC), C/Gran Capitá 2-4, Edif. Nexus 08034 Barcelona, Spain
[5] Facultad de Ciencias Astronómicas y Geofísicas, Universidad Nacional de La Plata, Paseo del Bosque, B1900FWA La Plata, Argentina
[6] Instituto de Astrofísica de La Plata (CCT-La Plata, CONICET-UNLP), Paseo del Bosque, B1900FWA La Plata, Argentina
[7] Department of Astrophysical Sciences, Princeton University, 4 Ivy Lane, Princeton, NJ 08544, USA
[8] Dept. of Physics, University of Warwick, Gibbet Hill Road, Coventry CV4 7AL, UK
[9] Center of Astro-Engineering UC, Pontificia Universidad Católica de Chile, Av. Vicuña Mackenna 4860, 7820436 Macul, Santiago, Chile
[10] Instituto de Astrofísica, Facultad de Física, Pontificia Universidad Católica de Chile, Av. Vicuña Mackenna 4860, 7820436 Macul, Santiago, Chile
[11] Millennium Institute of Astrophysics, Av. Vicuña Mackenna 4860, 782-0436 Macul, Santiago, Chile
[12] Observatoire des Baronnies provencales, Observatoire Astronomique, 05150 Moydans, France
[13] Observatory Puig d'Agulles, Carrer Riera 1, 08759 Vallirana, Spain
[14] Max-Planck-Institut für Astronomie, Königstuhl 17, 69117 Heidelberg, Germany
[15] NASA Goddard Space Flight Center, Exoplanets and Stellar Astrophysics Laboratory, Greenbelt, MD 20771, USA
[16] Emory University Department of Physics, 400 Dowman Drive, Suite N218,Atlanta, GA 30322, USA
[17] Kavli Institute for Astrophysics and Space Research, Massachusetts Institute of Technology, Cambridge, MA 02139, USA
[18] Rarotonga Observatory, PO Box 876, Rarotonga, Cook Islands
[19] La Vara, Valdes Observatory, 33784 Muñas de Arriba, Valdés, Asturias, Spain
[20] Yunnan Observatories, Chinese Academy of Sciences, Kunming 650011, PR China
[21] Key Laboratory for the Structure and Evolution of Celestial Objects, Chinese Academy of Sciences, Kunming 650216, PR China
[22] University of Chinese Academy of Sciences, Beijing 100049, PR China
[23] Observatori Astronòmic Albanyà, Camí de Bassegoda s/n, 17733 Albanyà, Spain
[24] Observatoire Astronomique de Vaison, 84110 Vaison la Romaine, France
[25] National Youth Space Center, 59567 Goheung, Jeollanam-do, South Korea
[26] Space Research Institute, Austrian Academy of Sciences, Schmiedlstr. 6, 8042 Graz, Austria
[27] Anunaki Observatory, Calle de los Llanos, 28410 Manzanares el Real, Spain
[28] School of Physical Sciences, The Open University, Milton Keynes MK7 6AA, UK
[29] Gruppo Astrofili Salese "Galileo Galilei", Via G. Ferraris 1, 30036 Santa Maria di Sala (VE), Italy
[30] Las Cumbres Observatory, 6740 Cortona Dr., Suite 102, Santa Barbara, CA 93117, USA
[31] Special Astrophysical Observatory, Russian Academy of Sciences, Nizhnij Arkhyz 369167, Russia
[32] Central Astronomical Observatory at Pulkovo of Russian Academy of Sciences, Pulkovskoje shosse d. 65, St., Petersburg 196140, Russia

Appendix A: Data reduction

The data reduction of the STELLA and CalarAlto data was done with a customized pipeline already used for previous transit light curve analyses (Mallonn et al. 2015, 2016; Mackebrandt et al. 2017). Aperture photometry was done with the publicly available software SExtractor (Bertin & Arnouts 1996). We selected the aperture size that minimized the scatter in the light curve residuals after subtraction of an initial transit model of literature transit parameters including a second-order polynomial over time for detrending. Using the same criterion of minimization of photometric scatter, our data reduction pipeline also automatically chose the best selection of comparison stars for differential photometry.

The TJO imaging frames were reduced using the ICAT reduction pipeline at the TJO (Colome & Ribas 2006) and aperture photometry was extracted using AstroImageJ.

The data reduction of the JST light curves was carried out using DIP2OL, which structure and use is fully explained in von Essen et al. (2018). Briefly, the first part of the pipeline is IRAF-based; it carries out the pre-reduction, the extraction of stellar fluxes, and the computation of photometric uncertainties in an automatized way. The second part of the pipeline is a python program that minimizes the scatter of the differential light curves by the most adequate combination of reference stars for the differential light curve, and an optimization of the aperture and the radius size where the sky counts are determined.

The four imaging time-series from the NYSC 1-m telescope were reduced by the IRAF *ccdred* package and aperture photometry was performed with SExtractor. Differential photometry was obtained by the usage of an ensemble of comparison stars.

The CHAT photometric images were reduced using a dedicated pipeline descendant of a pipeline created to obtain photometry using the Las Cumbres 1-m telescopes (Shporer et al. 2017; Espinoza et al., in prep.), which was also used for the LCO imaging time-series analyzed in this work.

The data reduction of the Yunnan Observatory data were reduced using the IRAF package, and systematic errors were removed from the resulting photometric data according to the procedures in Wang et al. (2014).

Appendix B: Figures and tables

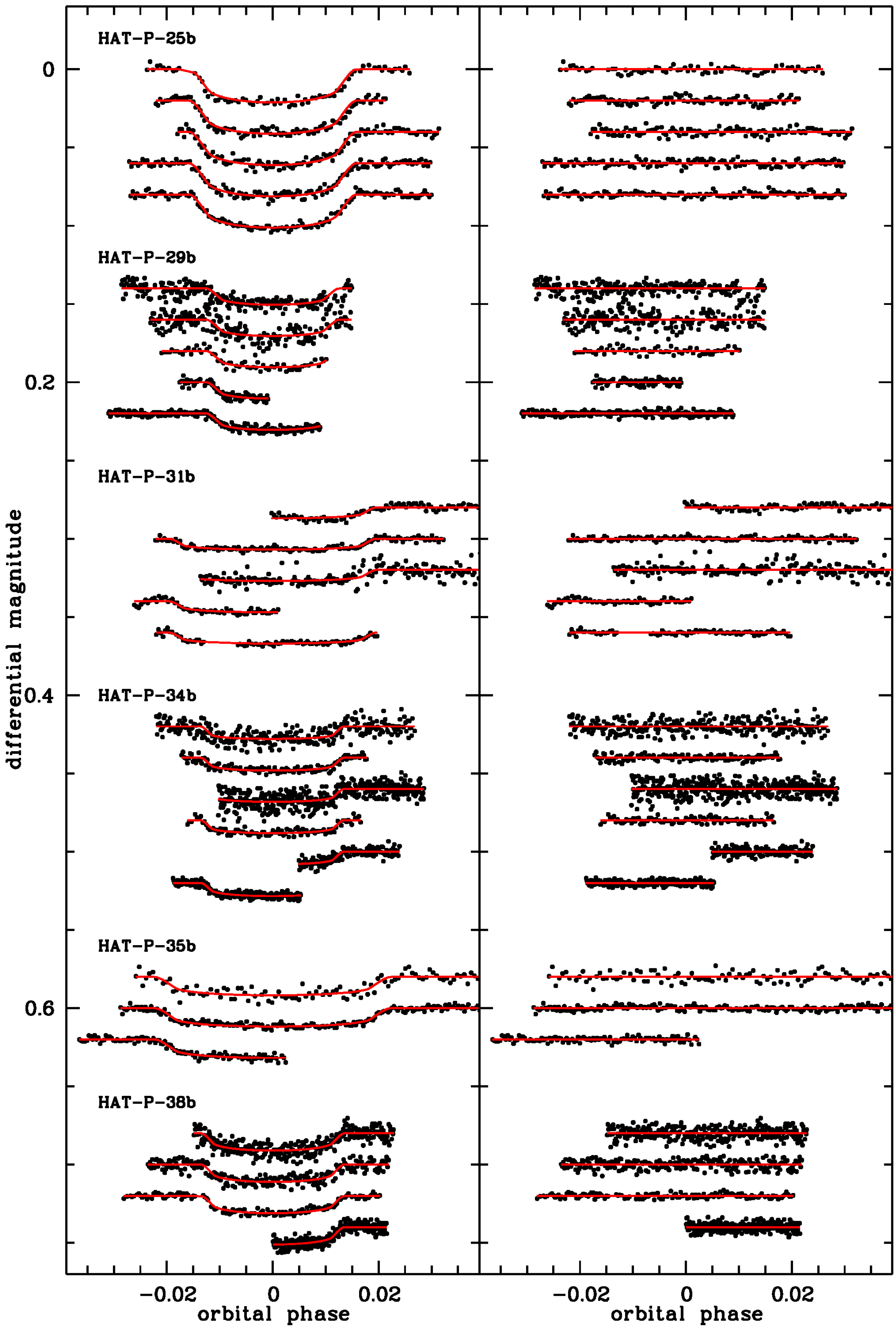

Fig. B.1. Detrended transit light curves in the same order as in Table B.1. Curves after the first are displaced vertically for clarity. Residuals from the fits are displayed in the right panel with the same vertical offset.

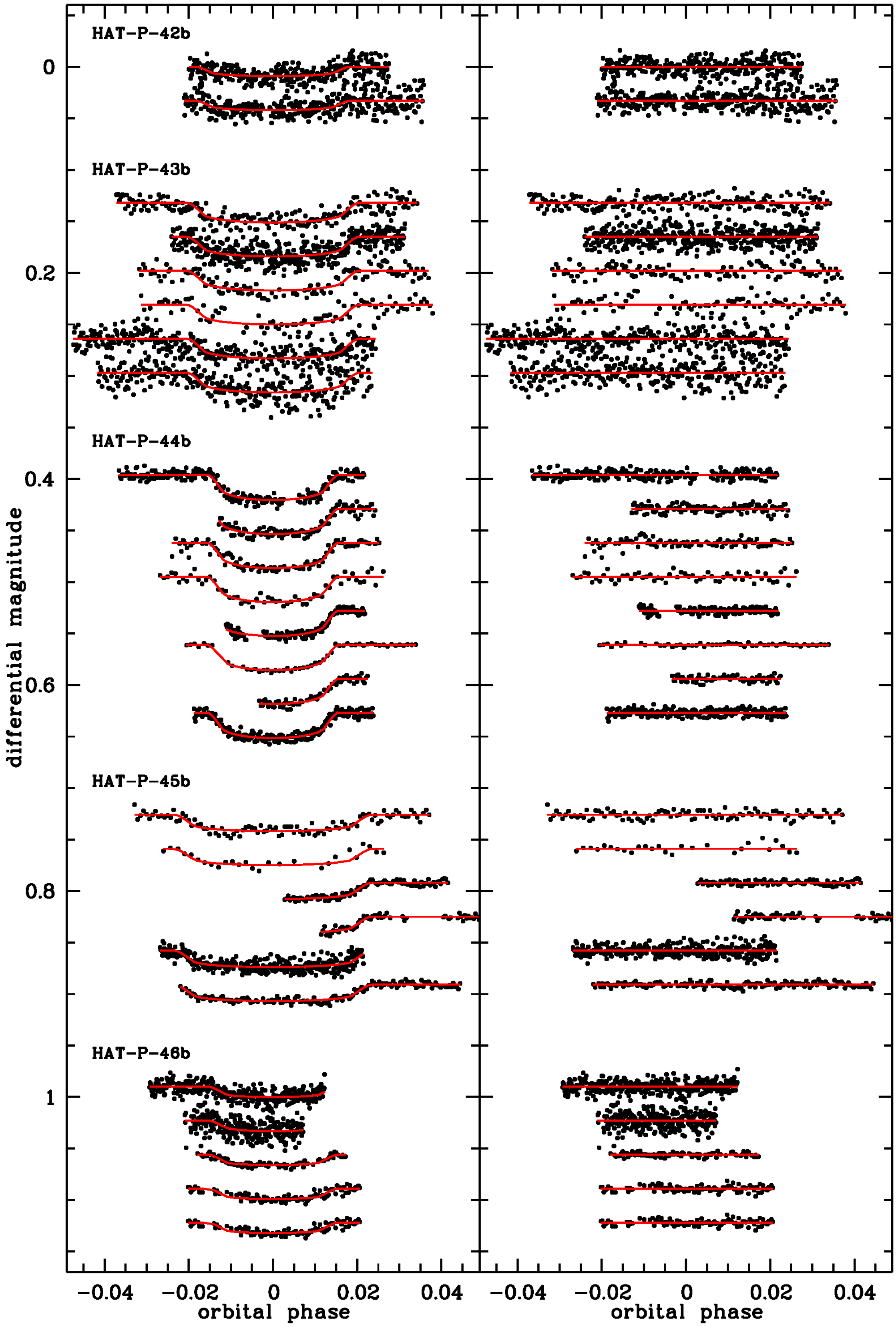

Fig. B.1. continued.

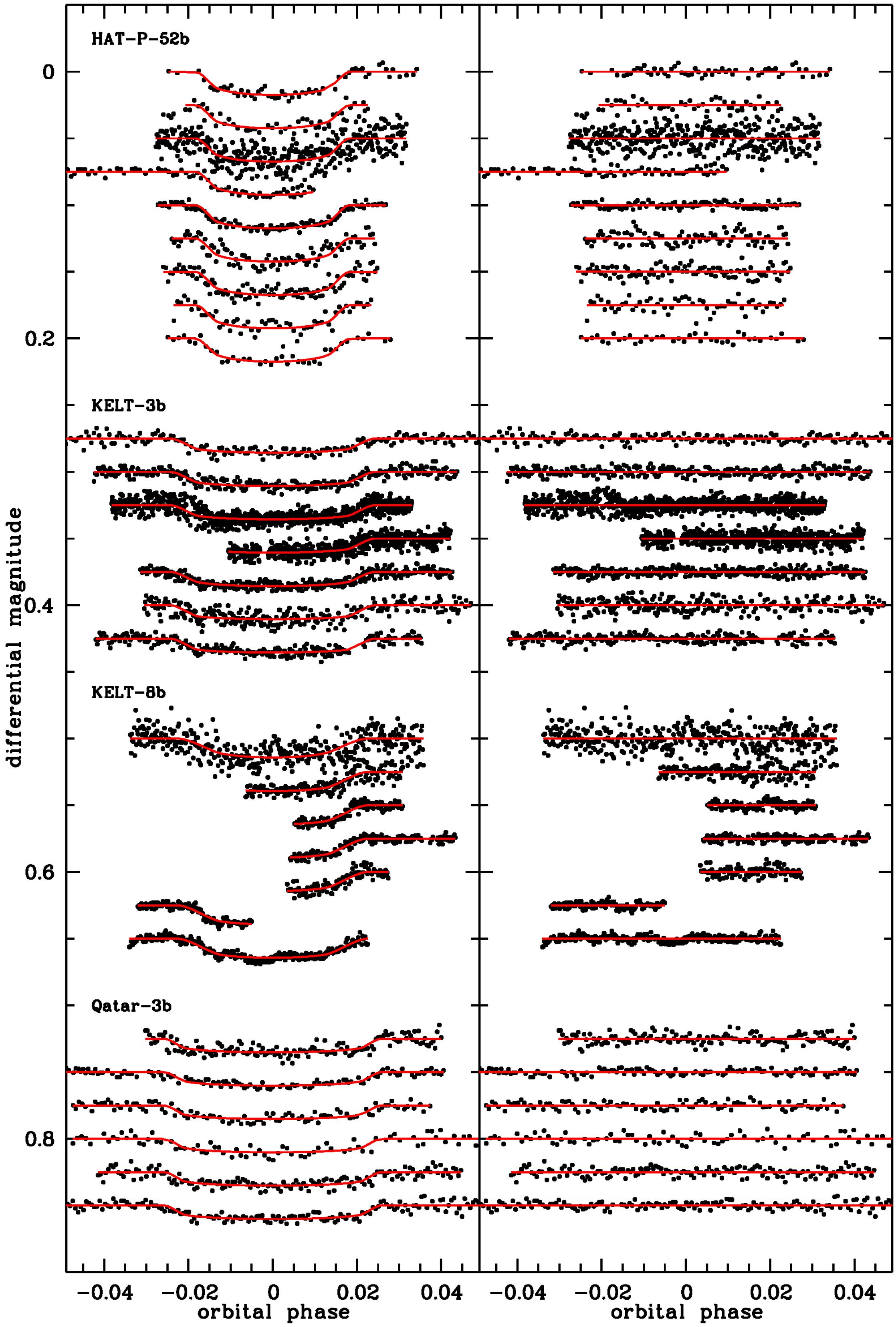

Fig. B.1. continued.

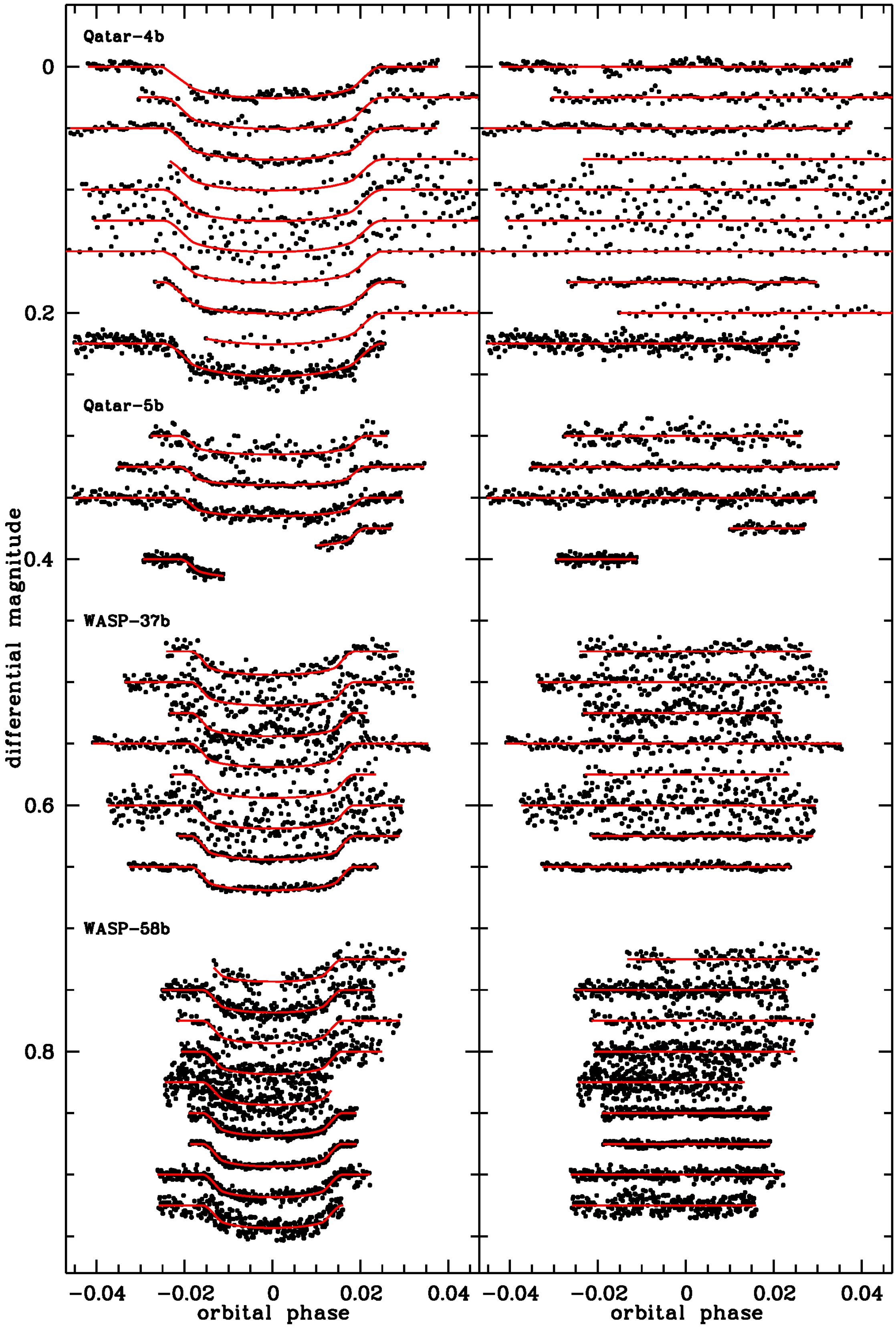

Fig. B.1. continued.

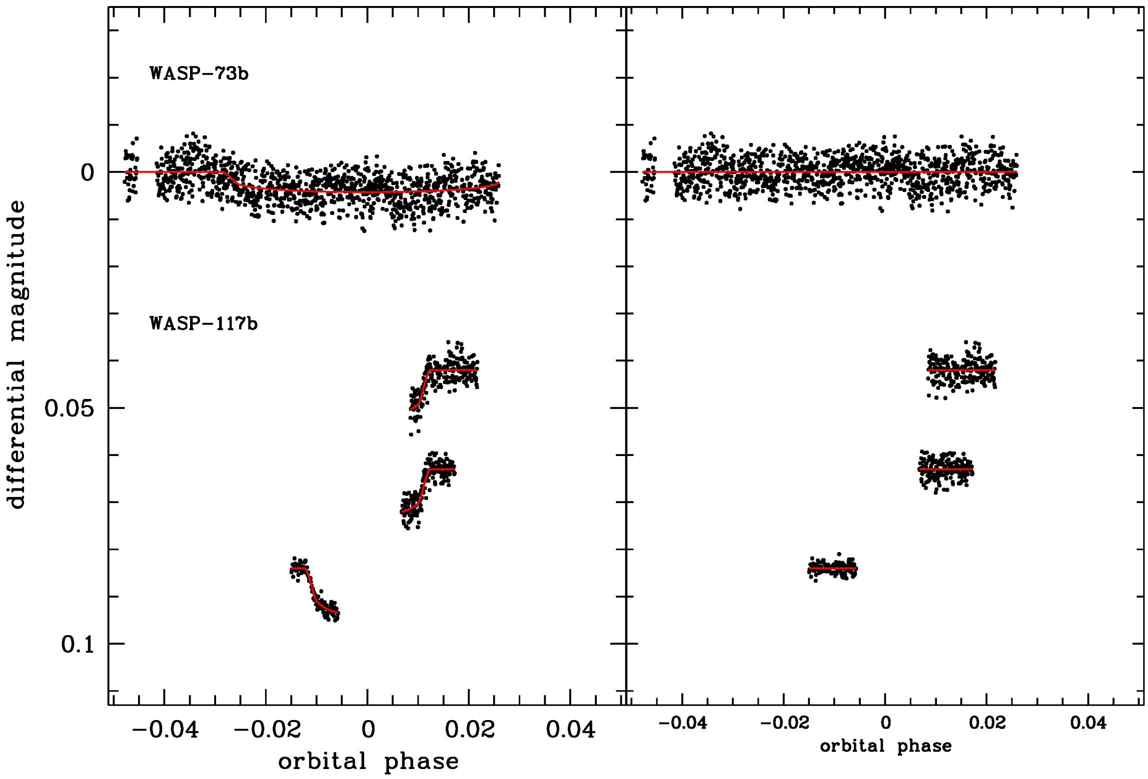

Fig. B.1. continued.

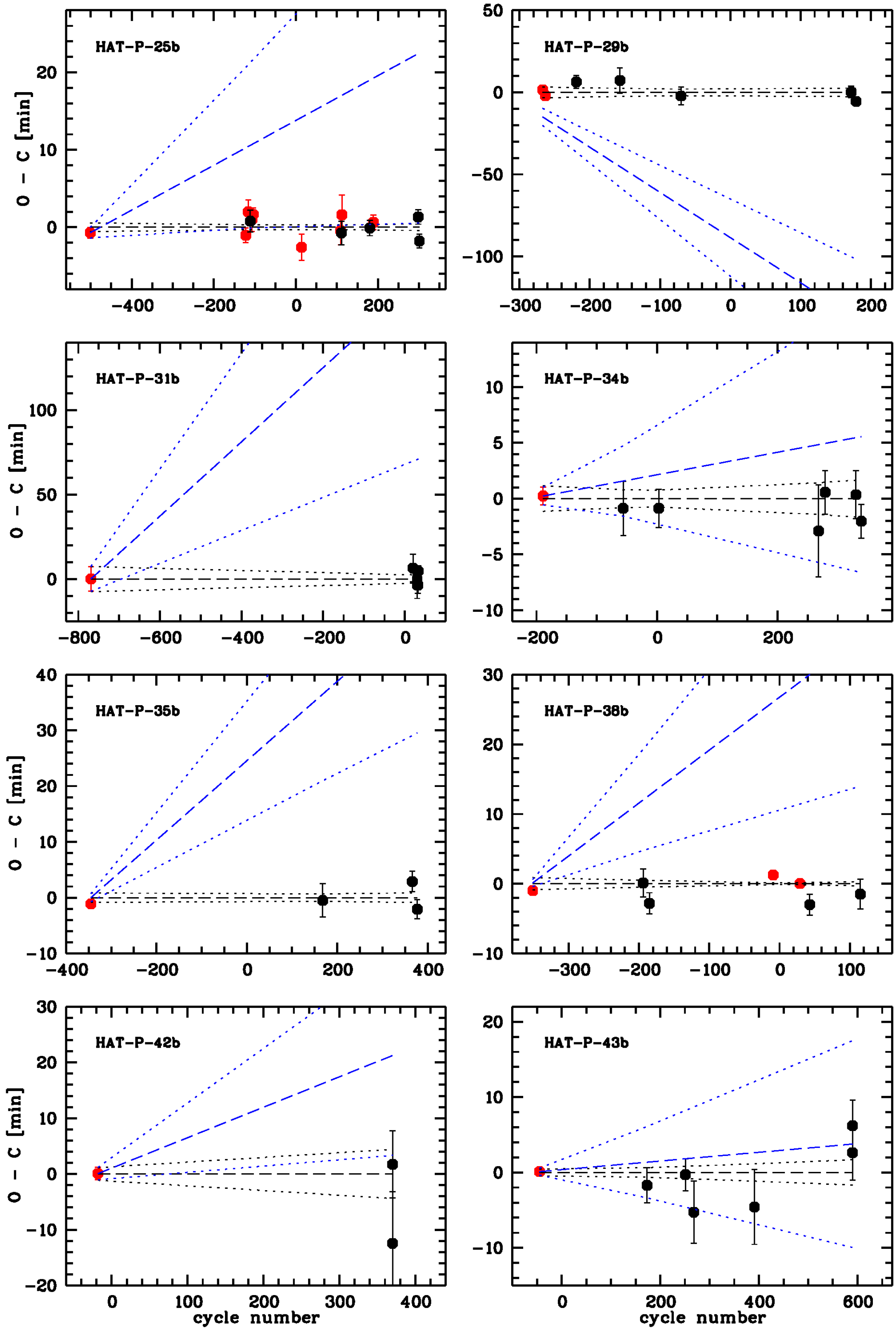

Fig. B.2. Observed minus calculated mid-transit times for HAT-P-25b, HAT-P-29b, HAT-P-31b, HAT-P-34b, HAT-P-35b, HAT-P-38b, HAT-P-42b, and HAT-P-43b. Measurements of this work in black, literature values included in our calculation in red. A black dashed line denotes the new ephemeris of this work with associated uncertainties in dotted lines. For comparison, the previous ephemeris of the discovery paper in blue. The offset between previous ephemeris and literature value for HAT-P-29b is caused by a timing offset corrected in Wang et al. (2018a); see text for details.

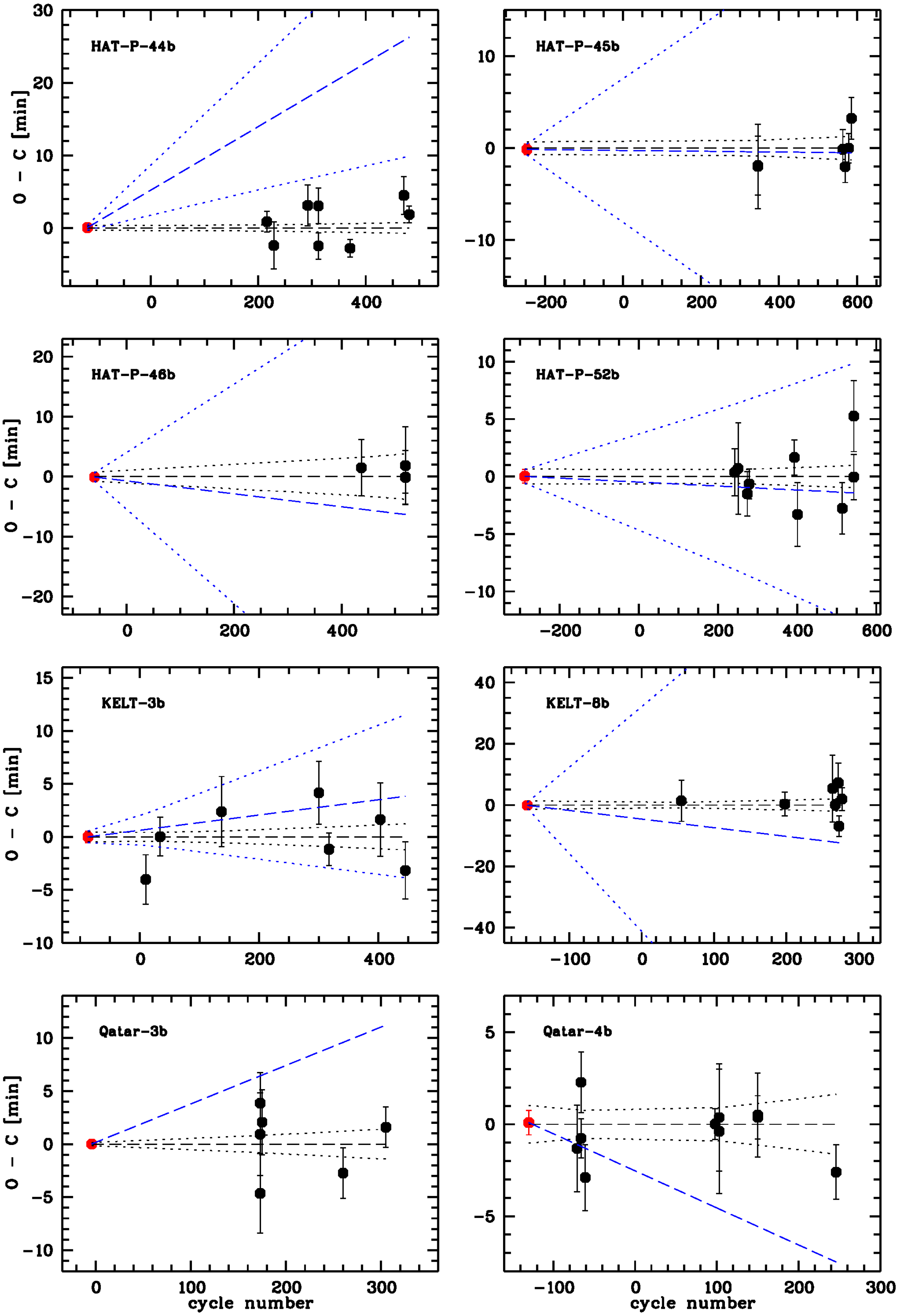

Fig. B.3. Continuation of Fig. B.2 for HAT-P-44b, HAT-P-45b, HAT-P-46b, HAT-P-52b, KELT-3b, KELT-8b, Qatar-3b, and Qatar-4b. We note that Qatar-3b and Qatar-4b lack an ephemeris uncertainty in their discovery paper.

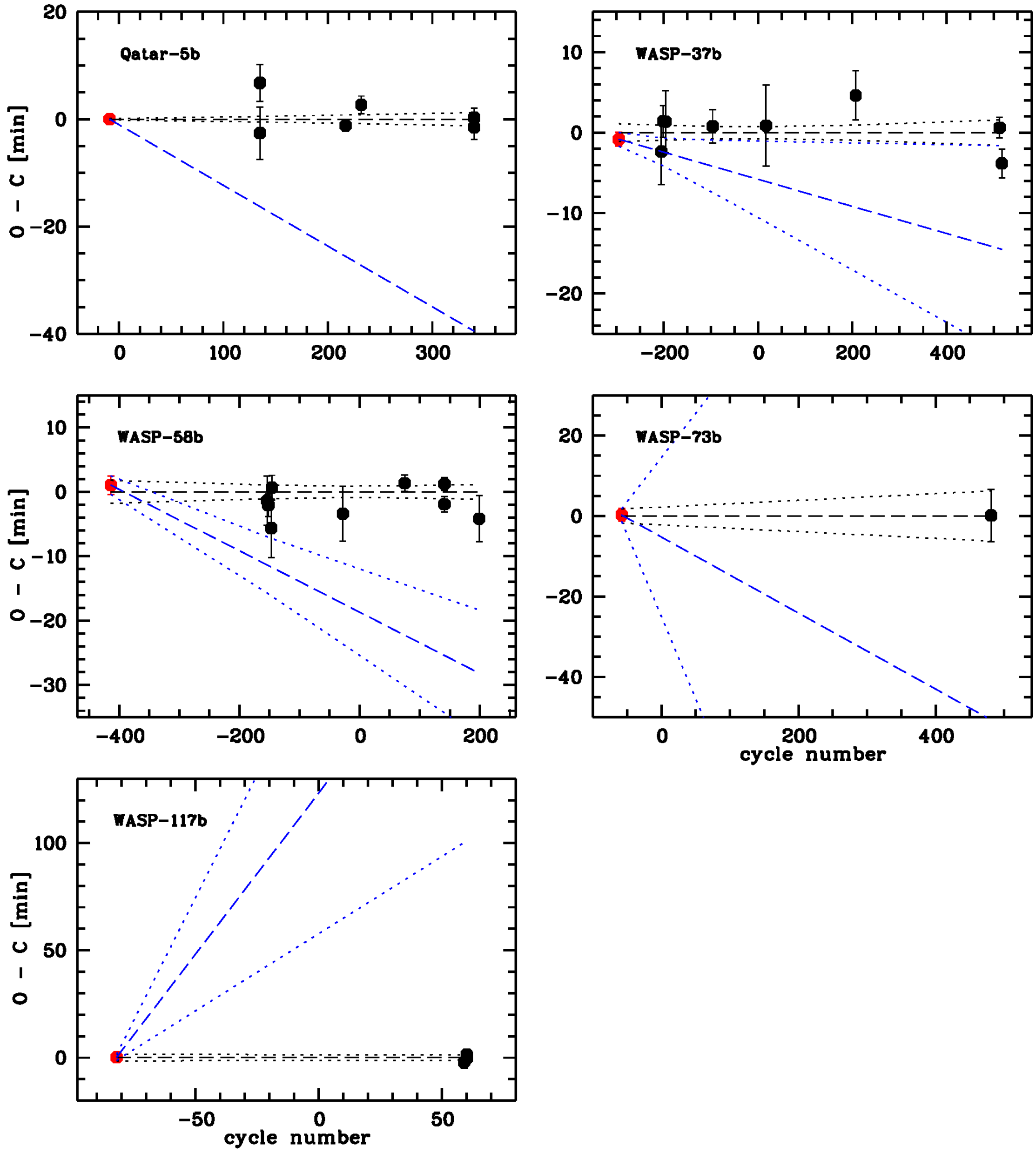

Fig. B.4. Continuation of Fig. B.2 for Qatar-5b, WASP-37b, WASP-58b, WASP-73b, and WASP-117b. We note that Qatar-5b lacks an ephemeris uncertainty in its discovery paper.

Table B.1. Overview about the transit observations of the investigated planets.

Planet	Date	Telescope	Filter	N_{data}	rms (mmag)	β
HAT-P-25b	2013, Nov 4	ETD, M. Salisbury	Clear	72	1.9	1.41
	2016, Jan 24	ETD, M. Bretton	Clear	102	2.0	2.01
	2016, Oct 2	ETD, V.-P. Hentunen	Clear	119	2.0	1.21
	2017, Dec 7	STELLA	r'	135	1.7	1.13
	2017, Dec 18	STELLA	r'	133	1.5	1.31
HAT-P-29b	2011, Oct 3	ETD, M. Vanhuysse	R	251	3.4	1.72
	2012, Sep 22	ETD, J. Trnka	Clear	204	4.6	1.51
	2014, Feb 2	ETD, M. Salisbury	R	61	1.8	1.22
	2017, Nov 18	STELLA	r'	88	1.6	1.48
	2017, Dec 28	STELLA	r'	239	1.3	1.00
HAT-P-31b	2018, May 31	NYSC 1m	R	111	1.6	2.03
	2018, Jul 20	NYSC 1m	R	129	1.1	1.28
	2018, Jul 20	Yunnan	R	253	3.3	1.06
	2018, Jul 30	NYSC 1m	R	65	1.4	1.46
	2018, Aug 04	NYSC 1m	R	84	1.1	1.38
HAT-P-34b	2012, Aug 17	ETD, S. Shadick	I	279	4.1	1.29
	2013, Jul 4	ETD, J. Gonzalez	Clear	126	1.5	1.01
	2017, Jun 18	ETD, F. Scaggiante	R	437	4.3	1.14
	2017, Aug 17	ETD, F. Campos	R	97	1.9	1.60
	2018, May 23	STELLA	r'	135	2.3	1.00
	2018, Jul 11	TJO	V	317	1.3	1.75
HAT-P-35b	2016, Mar 1	ETD, D. Molina	Clear	103	3.1	1.00
	2018, Feb 21	STELLA	r'	189	1.3	1.86
	2018, Apr 3	STELLA	r'	109	1.4	1.00
HAT-P-38b	2013, Oct 26	ETD, P. Benni	Clear	325	3.4	1.10
	2013, Dec 6	ETD, F. Garcia	Clear	227	2.8	1.00
	2016, Oct 29	ETD, M. Bretton	Clear	137	1.3	1.52
	2017, Sep 29	CalarAlto2.2m	R	286	2.4	1.28
HAT-P-42b	2016, Dec 31	ETD, F. Lomoz	Clear	322	6.5	1.33
	2016, Dec 31	ETD, F. Lomoz	Clear	367	7.5	1.04
HAT-P-43b	2014, Mar 7	ETD, P. Evans	Clear	200	5.7	1.11
	2014, Nov 22	ETD, P. Benni	Clear	432	7.3	1.05
	2015, Jan 17	ETD, J. Lozano	Clear	119	5.4	1.81
	2016, Mar 2	ETD, D. Molina	Clear	92	6.7	1.32
	2017, Dec 26	ETD, F. Lomoz	Clear	348	7.1	1.41
	2017, Dec 26	ETD, F. Lomoz	Clear	315	10.0	1.07
HAT-P-44b	2015, Apr 21	ETD, M. Salisbury	R	216	3.4	1.07
	2015, Jun 15	ETD, M. Salisbury	R	112	3.5	1.32
	2016, Mar 12	ETD, M. Bretton	Clear	93	3.8	1.70
	2016, Jun 6	ETD, A. Marchini	R	58	3.8	1.00
	2016, Jun 6	ETD, M. Raetz	Clear	164	2.5	1.31
	2017, Feb 15	NYSC 1m	R	53	1.1	1.28
	2018, Apr 21	ETD, Y. Jongen	Clear	66	2.5	1.17
	2018, Jun 3	ETD, Y. Ogmen	Clear	218	3.0	1.11
HAT-P-45b	2016, Jul 15	ETD, D. Molina	Clear	99	3.7	1.15
	2016, Jul 15	ETD, E. Diez Alonso	Clear	27	3.7	1.09
	2018, May 28	STELLA	r'	93	1.9	1.11
	2018, Jun 16	STELLA	r'	64	2.1	1.00
	2018, Jul 14	TJO	V	347	4.6	1.03
	2018, Aug 05	STELLA	r'	155	2.1	1.52
HAT-P-46b	2017, Jun 14	ETD, F. Lomoz	Clear	341	5.1	1.31
	2018, Jun 15	TJO	V	286	7.6	1.06
	2018, Jun 15	ETD, M. Bretton	I	90	1.7	1.36
	2018, Jun 15	ETD, Y. Jongen	Clear	98	2.6	1.23
HAT-P-52b	2015, Oct 16	ETD, P. Farissier	R	57	2.7	1.00
	2015, Nov 9	ETD, M. Bretton	Clear	43	3.9	1.18
	2016, Jan 12	ETD, P. Benni	Clear	389	8.3	1.00
	2016, Jan 25	ETD, M. Bretton	Clear	71	1.9	1.00
	2016, Dec 4	ETD, M. Bretton	Clear	102	1.9	1.66

Table B.1. continued.

Planet	Date	Telescope	Filter	N_{data}	rms (mmag)	β
	2016, Dec 26	ETD, M. Bretton	Clear	91	4.5	1.39
	2017, Nov 2	ETD, M. Bretton	*I*	97	4.0	1.35
	2018, Jan 21	ETD, D. Molina	Clear	57	4.6	1.00
	2018, Jan 21	ETD, F. Campos	Clear	40	2.3	1.00
KELT-3b	2013, Jan 4	ETD, R. Naves	R	215	2.9	1.00
	2013, Mar 9	ETD, A. Ayiomamitis	Clear	274	2.6	1.08
	2013, Dec 13	ETD, P. Benni	Clear	879	4.1	1.33
	2015, Feb 27	ETD, M. Salisbury	*R*	579	3.8	1.25
	2015, Apr 13	ETD, M. Bretton	*V*	358	2.3	1.24
	2015, Dec 2	ETD, S. Shadick	*I*	259	4.4	1.14
	2016, Mar 24	ETD, D. Molina	Clear	228	2.7	1.25
KELT-8b	2016, Jul 4	ETD, F. Lomoz	*B*	380	7.7	1.35
	2017, Oct 11	STELLA	r'	174	4.0	1.04
	2018, May 13	STELLA	r'	125	2.4	1.97
	2018, May 26	STELLA	r'	172	1.8	1.12
	2018, Jun 8	STELLA	r'	113	3.2	1.40
	2018, Jun 11	STELLA	r'	186	1.9	1.90
	2018, Jun 24	STELLA	r'	272	2.2	2.18
Qatar-3b	2016, Dec 23	ETD, W. Czech	Clear	147	3.7	1.36
	2016, Dec 23	ETD, M. Bretton	Clear	120	1.9	1.92
	2016, Dec 23	ETD, M. Bretton	Clear	98	2.6	1.27
	2016, Dec 28	ETD, Suricate48	Clear	78	3.4	1.00
	2017, Jul 30	ETD, M. Morales	Clear	143	3.2	1.13
	2017, Nov 19	ETD, P. Guerra	Clear	179	2.9	1.01
Qatar-4b	2016, Dec 21	ETD, M. Bretton	Clear	156	2.9	2.41
	2016, Dec 30	ETD, M. Bachschmidt	Clear	100	3.1	1.00
	2016, Dec 30	ETD, M. Bretton	Clear	104	2.5	2.24
	2017, Jan 8	ETD, F. Garcia	Clear	48	3.1	1.00
	2017, Oct 22	ETD, M. Salisbury	*R*	43	1.8	1.00
	2017, Oct 31	ETD, V.-P. Hentunen	*R*	146	6.4	1.70
	2017, Oct 31	ETD, V.-P. Hentunen	Clear	136	9.2	1.30
	2018, Jan 24	ETD, M. Bretton	*I*	72	2.0	1.35
	2018, Jan 24	ETD, F. Campos	Clear	42	3.1	1.00
	2018, Jul 16	TJO	*V*	307	4.7	1.25
Qatar-5b	2016, Dec 28	ETD, M. Bachschmidt	Clear	131	5.9	1.23
	2016, Dec 28	ETD, M. Bretton	Clear	104	3.8	1.37
	2017, Aug 21	ETD, M. Bretton	*I*	136	1.8	1.24
	2017, Oct 4	ETD, K. Fenzl	*R*	243	3.5	1.31
	2018, Aug 10	STELLA	r'	46	2.4	1.00
	2018, Aug 10	TJO	*V*	126	2.5	1.11
WASP-37b	2011, Apr 9	ETD, J.A. Carrion	R	124	5.1	1.44
	2011, Apr 23	ETD, K. Hose	*R*	186	5.3	1.00
	2011, May 11	ETD, S. Shadick	Clear	201	6.4	1.52
	2012, May 3	ETD, A. Carreno	Clear	169	3.6	1.20
	2013, Jun 11	ETD, R. Majewski	Clear	57	6.1	1.00
	2015, Apr 22	ETD, J. Trnka	Clear	274	8.6	1.02
	2018, Apr 17	STELLA	r'	137	1.5	1.18
	2018, May 5	STELLA	r'	154	1.7	2.03
WASP-58b	2013, Jul 14	ETD, J. Mravik	Clear	125	5.1	1.00
	2013, Jul 24	ETD, A. Ayiomamitis	Clear	273	4.2	1.00
	2013, Aug 19	ETD, F.G. Horta	*V*	123	5.4	1.58
	2013, Aug 24	ETD, J.L. Martin	*V*	251	4.8	1.04
	2015, Apr 8	ETD, M. Bretton	*R*	338	8.4	1.21
	2016, Sep 5	ETD, V.-P. Hentunen	*R*	243	2.3	1.11
	2017, Aug 2	ETD, M. Bretton	*I*	232	1.6	1.53
	2017, Aug 2	ETD, R. Ballet	Clear	304	3.1	1.10
	2018, May 20	ETD, M. Hoecherl	*V*	295	5.4	1.38
WASP-73b	2018, Aug 01	JST	*R*	1177	3.1	1.75

Table B.1. continued.

Planet	Date	Telescope	Filter	N_{data}	rms (mmag)	β
WASP-117b	2017, Jul 12	CHAT	i'	215	2.1	1.24
	2017, Jul 22	CHAT	i'	184	1.7	1.00
	2017, Jul 22	LCO	i'	109	1.0	1.00

Table B.2. Observed transit times of the investigated planets.

Planet	BJD(TDB) (2 450 000+)	Epoch	Reference
HAT-P-25b	5176.85173 ± 0.00047	−501	Quinn et al. (2012)
	6561.26872 ± 0.00066	−122	Wang et al. (2018b)
	6583.18773 ± 0.00105	−116	Wang et al. (2018b)
	6601.45096 ± 0.00097	−111	This work
	6616.06236 ± 0.00106	−107	Wang et al. (2018b)
	6627.02128 ± 0.00058	−104	Wang et al. (2018b)
	7058.05061 ± 0.00119	14	Wang et al. (2018b)
	7405.06961 ± 0.00125	109	Wang et al. (2018b)
	7412.37504 ± 0.00105	111	This work
	7416.02949 ± 0.00178	112	Wang et al. (2018b)
	7664.41978 ± 0.00068	180	This work
	7697.29563 ± 0.00065	189	Wang et al. (2018b)
	8095.45305 ± 0.00064	298	This work
	8106.40933 ± 0.00062	301	This work
HAT-P-29b	5563.87156 ± 0.00065	−267	Wang et al. (2018a)
	5586.76257 ± 0.00061	−263	Wang et al. (2018a)
	5838.59183 ± 0.00325	−219	This work
	6193.43030 ± 0.00402	−157	This work
	6691.36248 ± 0.00266	−70	This work
	8076.42237 ± 0.00244	172	This work
	8116.48552 ± 0.00126	179	This work
HAT-P-31b	4320.8866 ± 0.0051	−769	Kipping et al. (2011)
	8270.05094 ± 0.00564	20	This work
	8320.09907 ± 0.00131	30	This work
	8320.09673 ± 0.00550	30	This work
	8330.10726 ± 0.00340	32	This work
	8335.11829 ± 0.00213	33	This work
HAT-P-34b	5431.59706 ± 0.00055	−189	Bakos et al. (2012)
	6156.78867 ± 0.00313	−56	This work
	6478.49205 ± 0.00136	3	This work
	7923.44147 ± 0.00381	268	This work
	7983.42395 ± 0.00406	279	This work
	8261.50682 ± 0.00183	330	This work
	8310.60566 ± 0.00140	339	This work
HAT-P-35b	5578.66081 ± 0.00050	−345	Bakos et al. (2012)
	7449.39606 ± 0.00207	168	This work
	8171.43644 ± 0.00127	366	This work
	8211.54620 ± 0.00118	377	This work
HAT-P-38b	5863.11957 ± 0.00035	−351	Sato et al. (2012)
	6591.65204 ± 0.00139	−194	This work
	6633.41297 ± 0.00106	−185	This work
	7450.11375 ± 0.00045	−9	Bruno et al. (2018)
	7626.44542 ± 0.00010	29	Bruno et al. (2018)
	7691.40793 ± 0.00103	43	This work
	8025.51268 ± 0.00149	115	This work
HAT-P-42b	5952.52683 ± 0.00077	−18	Boisse et al. (2013)
	7753.55133 ± 0.00639	370	This work
	7753.56116 ± 0.00417	370	This work

Table B.2. continued.

Planet	BJD(TDB) (2 450 000+)	Epoch	Reference
HAT-P-43b	5997.37182 ± 0.00032	−45	Boisse et al. (2013)
	6723.89545 ± 0.00162	173	This work
	6983.84571 ± 0.00148	251	This work
	7040.49786 ± 0.00287	268	This work
	7450.41836 ± 0.00345	391	This work
	8113.62728 ± 0.00255	590	This work
	8113.62975 ± 0.00236	590	This work
HAT-P-44b	5696.93772 ± 0.00024	−118	Hartman et al. (2014)
	7133.53528 ± 0.00100	216	This work
	7189.44845 ± 0.00226	229	This work
	7460.42717 ± 0.00194	292	This work
	7546.45090 ± 0.00172	312	This work
	7546.44706 ± 0.00127	312	This work
	7800.21697 ± 0.00083	371	This work
	8230.34088 ± 0.00180	471	This work
	8273.35095 ± 0.00081	481	This work
HAT-P-45b	5729.98689 ± 0.00041	−247	Hartman et al. (2014)
	7585.47810 ± 0.00222	346	This work
	7585.47804 ± 0.00319	346	This work
	8267.59965 ± 0.00148	564	This work
	8286.37230 ± 0.00120	570	This work
	8314.53462 ± 0.00110	579	This work
	8336.43982 ± 0.00159	586	This work
HAT-P-46b	5701.33723 ± 0.00047	−60	Hartman et al. (2014)
	7919.51715 ± 0.00326	437	This work
	8285.49459 ± 0.00451	519	This work
	8285.49325 ± 0.00184	519	This work
	8285.49321 ± 0.00312	519	This work
HAT-P-52b	5852.10403 ± 0.00041	−288	Hartman et al. (2015)
	7311.51042 ± 0.00142	242	This work
	7336.29302 ± 0.00277	251	This work
	7399.62421 ± 0.00133	274	This work
	7413.39279 ± 0.00091	279	This work
	7727.30439 ± 0.00107	393	This work
	7749.32972 ± 0.00193	401	This work
	8060.48649 ± 0.00155	514	This work
	8140.34636 ± 0.00214	543	This work
	8140.34268 ± 0.00137	543	This work
KELT-3b	6034.29537 ± 0.00038	−87	Pepper et al. (2013)
	6296.52093 ± 0.00162	10	This work
	6361.40497 ± 0.00127	34	This work
	6639.85526 ± 0.00230	137	This work
	7080.50825 ± 0.00205	300	This work
	7126.46210 ± 0.00106	317	This work
	7358.95516 ± 0.00240	403	This work
	7472.49400 ± 0.00188	445	This work
KELT-8b	6883.4803 ± 0.0007	−158	Fulton et al. (2015)
	7574.47027 ± 0.00464	55	This work
	8038.37293 ± 0.00268	198	This work
	8252.4856 ± 0.0076	264	This work
	8265.45835 ± 0.00121	268	This work
	8278.43966 ± 0.00446	272	This work
	8281.67389 ± 0.00234	273	This work
	8294.65635 ± 0.00258	277	This work
Qatar-3b	7302.45300 ± 0.00010	−4	Alsubai et al. (2017)
	7746.34721 ± 0.00260	173	This work
	7746.35109 ± 0.00272	173	This work
	7746.35313 ± 0.00201	173	This work

Table B.2. continued.

Planet	BJD(TDB) (2,450,000+)	Epoch	Reference
	7751.36766 ± 0.00214	175	This work
	7964.53543 ± 0.00165	260	This work
	8077.39371 ± 0.00132	305	This work
Qatar-4b	7637.77361 ± 0.00046	−130	Alsubai et al. (2017)
	7744.28950 ± 0.00164	−71	This work
	7753.31672 ± 0.00074	−66	This work
	7753.31884 ± 0.00115	−66	This work
	7762.34209 ± 0.00125	−61	This work
	8049.39801 ± 0.00058	103	This work
	8058.42511 ± 0.00203	103	This work
	8058.42459 ± 0.00235	98	This work
	8143.27752 ± 0.00082	150	This work
	8143.27761 ± 0.00159	150	This work
	8316.59101 ± 0.00103	246	This work
Qatar-5b	7336.75824 ± 0.00010	−9	Alsubai et al. (2017)
	7751.37715 ± 0.00338	135	This work
	7751.38365 ± 0.00240	135	This work
	7987.48158 ± 0.00074	217	This work
	8030.67394 ± 0.00113	232	This work
	8341.63656 ± 0.00154	340	This work
	8341.63779 ± 0.00127	340	This work
WASP-37b	5338.6196 ± 0.0006	−295	Simpson et al. (2011)
	5660.59180 ± 0.00284	−205	This work
	5674.90434 ± 0.00138	−201	This work
	5692.79172 ± 0.00267	−196	This work
	6050.53938 ± 0.00145	−96	This work
	6454.79476 ± 0.00348	17	This work
	7134.51870 ± 0.00211	207	This work
	8225.64753 ± 0.00892	512	This work
	8243.53184 ± 0.00125	517	This work
WASP-58b	5183.9342 ± 0.0010	−414	Hébrard et al. (2013)
	6488.40794 ± 0.00264	−154	This work
	6498.44187 ± 0.00121	−152	This work
	6523.52545 ± 0.00316	−147	This work
	6528.54704 ± 0.00134	−146	This work
	7120.57537 ± 0.00297	−28	This work
	7637.35161 ± 0.00089	75	This work
	7968.48759 ± 0.00068	141	This work
	7968.48541 ± 0.00082	141	This work
	8259.48221 ± 0.00249	199	This work
WASP-73b	6128.7063 ± 0.0011	−58	Delrez et al. (2014)
	8331.7531 ± 0.0045	481	This work
WASP-117b	6533.82404 ± 0.00095	−82	Lendl et al. (2014)
	7946.72810 ± 0.00198	59	This work
	7956.74985 ± 0.00163	60	This work
	7956.75113 ± 0.00105	60	This work